Strong Ground Motion Simulation of the 2017 Sefid-Sang Earthquake in Khorasan-Razavi, NE Iran

Hesaneh Mohammadi [1*], Maryam Sedghi [2], Mohammad Reza Gheitanchi [3]

[1*] *PhD Candidate, Geophysics Department, Tehran North Branch, Islamic Azad University, Tehran, Iran*

(h.mohammadi@iau-tnb.ac.ir)

[2] *senior expert in research, Iranian Red Crescent Society (IRCS), Tehran, Iran*

[3] *Professor, Institute of Geophysics, University of Tehran, Tehran, Iran*

ABSTRACT

On April 5, 2017, an earthquake with moment magnitude of 6.1 occurred Sefid-Sang area about 80 km southeast of Mashhad city in Khorasan-e-Razavi province. In this study, to estimate source parameters and rupture characteristics of the earthquake, the Empirical Green Function (EGF) method and the stochastic finite-fault (SFF) technique were used for strong ground motion simulation. Then the observed records and the simulated graphs by these two methods, were compared. To simulate the earthquake by EGF method, an aftershock with moment magnitude of 4.8 was used as the empirical Green function. The size of the main fault caused by the event was about 10 km in length and 8 km in width. The duration of the rupture in this event was about 18 seconds. The estimated fault plane solution shows reverse mechanism with strike-slip component. Strike, dip and rake of causative fault of the earthquake were determined as 311, 55 and 117 degrees. In addition, the stress drop in this event was calculated to be about 8 bars.

Keywords:

1. Introduction

Iran is located in the middle-east, along the Alpine-Himalayan active mountain belt. Continental convergence between Arabia and Eurasia plates caused seismic deformation in Iran; as a result of the deformation associated with the collision, several tectonic features were formed such as Zagros fold and thrust belt under the Caspian Sea. The historical background and instrumentally recorded earthquakes in the last two centuries indicate that Iran is seismically active but the rate of activity in Iran is not uniformly distributed and changes from place to place. In Alborz region and central Iran several destructive earthquakes were recorded in the past two decades, the earthquakes in these regions are shallow and produce high intensity. In most cases large events are accompanied by surface rupture; therefore, destructions during these earthquakes are considerable.

On April 5, 2017, an earthquake with moment magnitude of 6.1 occurred in Sefid Sang, southeast of Mashhad city in khorasan- Razavi province, which is one of the most seismically active regions in the country. This province is surrounded by branches of the active Kashafrud and Tous faults (Berberian 1983) [1]; Tous fault is a branch of Kashafrud fault that has a northwest-southeast trend and was first introduced by Berberian et al. (2000) [2] based on geomorphologic evidence (Arjmand et al. 2019) [3]. Study of historical and instrumental earthquakes (after 1900) suggests a high seismicity potential of the area. The seismicity map of Khorasan- Razavi is shown in Figure 1.
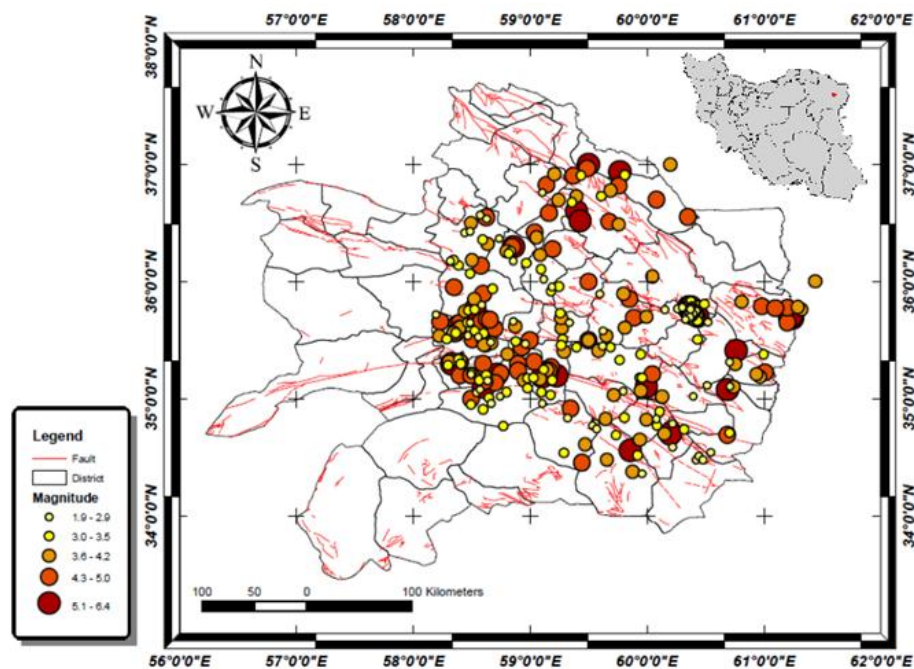

Figure 1. The seismicity map of Khorasan- Razavi province.

Sefid Sang earthquake has been recorded by 19 accelerometer stations of Iran Strong Motion Network (ISMN). In this paper, in order to estimate source parameters and rupture process of the earthquake, the Empirical Green Function method and the stochastic finite-fault technique were applied to simulate strong ground motion. These techniques permit estimation of parameters such as seismic moment, corner frequency, and source duration and rupture characteristics of the earthquake (Miyake et al. 2000) [4]. These methods have been widely used in Iran to simulate earthquakes in different regions such as 2005 Zarand earthquake by Zafarani (2012) [5], 2004 Firozabad Kojoor earthquake by Rahimi-Bahoosh and Hamzehloo (2011) [6].

2. Data Analysis

Ground motions recorded at radii less than 10 degrees from fault dimensions are called near source data. Near source ground motion records contain better signatures of spatial and temporal distribution of slip since these are highly influenced by the seismic source effects such as directivity, near source pulse motion and static offsets (Kanth 2008) [7]. In this study, near source data recorded by 19 accelerometers were used to estimate source parameters. All of the SSA-2 strong motion instruments that recorded this event have the trigger threshold of 10 cm/s2. This means that if the acceleration of the earthquake on any of the three components of the instrument reaches to this limit, the instrument starts to record the event. Also the accelerogram registered at Nasrabad station is one of the most important recorded accelerograms in terms of the maximum acceleration. Before using accelerograms, data processing is necessary; it includes baseline correction and filtering. By a linear correction, the divergence from the base line was resolved; also by 4th order of Butterworth filter the data were filtered, this filtering helped baseline correction too. In order to calculate the stress drop for this event, the corner frequency and seismic moment were determined using Fourier Spectrum in logarithmic scale. Using their values, the stress drop was estimated. The parameters estimated from the Fourier spectra, are shown in table 1. Using Peak Ground Accelerations (PGA) recorded by 19 near- field stations, the distribution of PGAs, corresponds to the event was estimated. The Spatial distribution of PGAs corresponding to the Sefid Sang earthquake is demonstrated in Figure 2.

Table1. The parameters estimated from the Fourier spectra.

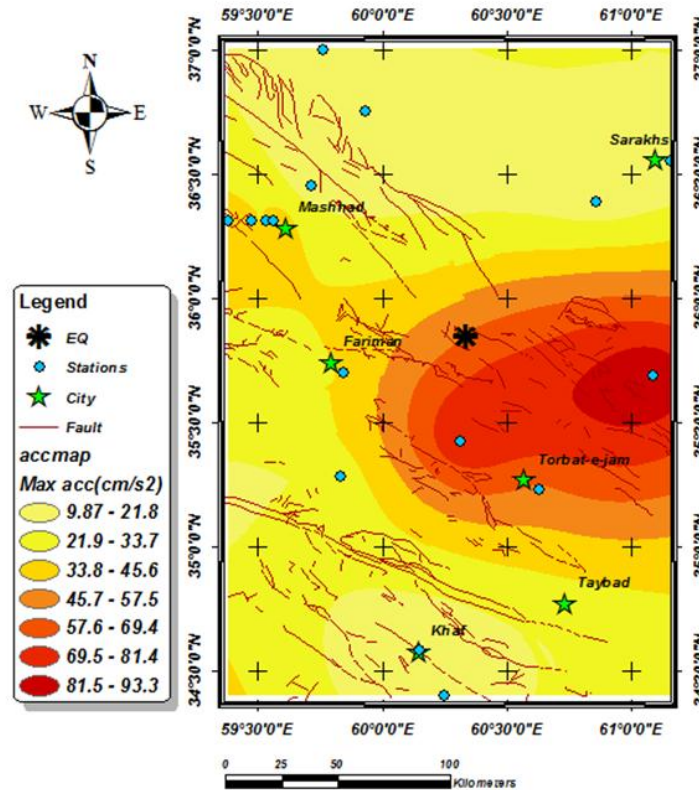|	Corner frequency(*HZ*)	Seismic moment(*N.M*)	Stress drop(*BAR*)
Main event	0.6	9.81×10^{17}	8

Figure 2. Spatial distribution of PGAs corresponding to the Sefid Sang earthquake.

3. The Empirical Green Function

In the present paper, to estimate source parameters and rupture process of the earthquake, Empirical Green Function (EGF) method was applied. EGF method suggested by Hartzell (1978) [8] is one of the most popular and widely used methods in simulating strong ground motions. This method has been widely applied to a large number of earthquakes ranging from moderate (M=5) to very large (M=8) events, using local network data. Over the last couple of decades, empirical Green functions have been increasingly used in earthquake source studies, crustal attenuation studies, strong ground motion prediction, finite rupture modelling, and site-response studies (Mueller 1985) [9]. Theoretically, Green functions are the impulse response of the medium, and EGFs are recordings used to provide this impulse response (Hutchings and Viegas 2012) [10]. In this technique, to simulate the target (main) event, an element event is used. Element (small) event is a foreshock or aftershock of the earthquake (Cheng and Huang 2011) [11]. The empirical Green function method shows that recordings of small events contain the propagation characteristics which are necessary for modelling large nearby earthquakes and therefore yield empirical Green functions are more appropriate than the synthetic seismograms generated by modelling the wave propagation in an inadequately known structure (Courboulex et al. 1996) [12]. Using small earthquakes to provide EGF for synthesizing larger earthquakes is very practical; small earthquakes occur hundreds of times more frequently than larger earthquakes and EGF can be readily obtained in a short period of time before a large earthquake occurs. The EGF method assumes that the two events have the same hypocenter. Consequently, waves that radiate from the nucleation points of the two events should cross exactly the same medium (Courboulex et al. 1996). To find small

event for which this technique can be applied, several criteria were defined. In the search for potential candidate of Sefid Sang earthquake, the following criteria were used: The difference in magnitudes must be larger or equal to 1. Both events must be recorded at a minimum of three common stations. The stations must be well distributed in azimuth around the epicentre. The epicentre of small event must be located as close as possible to that of the main event. In this study, an aftershock with moment magnitude of 4.8 was selected as the empirical Green function for the main earthquake. The focal mechanism of the element event should be similar to that of the target event (Irikura 1991) [13], so that the aftershock used as the empirical Green function, has the focal mechanism (Strike: 304º, Dip: 49º, Rake: 134 º) similar to that of the main event (Strike: 329 º, Dip: 45º, Rake: 127º). The focal mechanisms of the earthquake (target event) and its aftershock (element event) selected as Green function, are shown in Figure 3. Also the distribution of about 400 aftershocks and the location of the five stations at which both target and element events were recorded are demonstrated in this Figure.
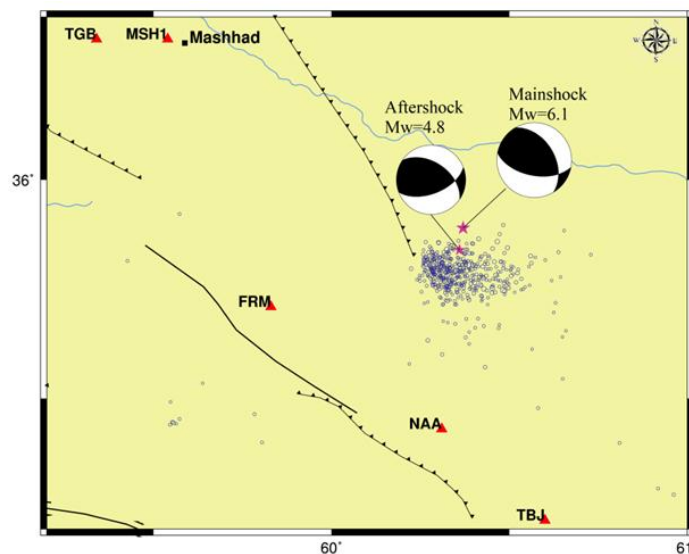

Figure 3. The distribution of aftershocks; the focal mechanisms of the target and small event selected as Green function and five common stations at which both events were recorded.

In this technique, the fault plane of main shock is divided in to sub faults of equal size. The size of the main fault and sub faults corresponds to the rupture area of main event and small event, respectively. In this study, the fault rupture dimensions were calculated using the equations estimated by Wells and Coppersmith (1994) [14]. The parameters of fault rupture generated during this event are shown in table 2. Also, the causative fault plane model of the main event is shown in Figure 4. Using this fault rupture model, strong ground motion simulation was carried out; it means, the values which are obtained, depend on the kinematic model that is used.

Table 2. The parameters of the fault plane.

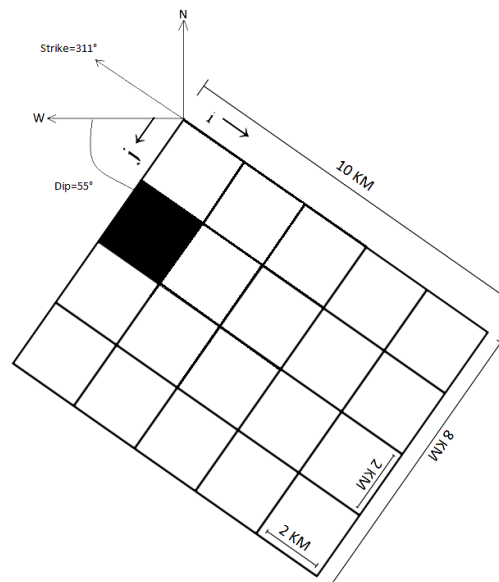| Fault length in strike direction (KM)	Fault length in dip direction (KM)	Sub fault length(KM)	Sub fault width(KM)	Number of elements in strike direction	Number of elements in dip direction
10	8	2	2	5	4

Figure 4. The causative fault plane model of the earthquake.

In this study, EGF algorithm (Irikura 1983) [15] was used to simulate the ground motions. Based on the source model, the synthetic waveforms of the small event were selected as the input motions to simulate the main shock records using the summation procedure of the EGF method (Irikura 1986) [16]; it means Green functions are summed up along the rupture propagation to generate strong ground motion.

4. Stochastic Finite Fault Method

Stochastic models of the seismic source and wave propagation have been used to simulate ground motions for many years (e.g., Boore 1983, 2003) [17-18]. The conventional point source approximation is unable to characterize key features of ground motions from large earthquakes, such as their long duration and the dependence of amplitudes and duration on the azimuth to the observation point (source directivity). Furthermore, finite source model is used to simulate the ground motion that contributes not only to the duration and directivity of ground motions, but also affect the shape of the spectra of seismic waves. The finite-fault stochastic modelling is achieved by stacking all the contributions from point source simulations at a number of sub faults distributed over the entire fault-rupture surface with appropriate time delay (Sengupta 2012) [19]. The

modelling considers fault-rupture dimensions, focal mechanism, seismic moment or magnitude, stress drop, slip distribution, hypocentral distance (or epicentral distance), focal depth, and fault pulsing percentage. The stochastic simulation technique developed by Motazedian and Atkinson (2005) [20] is employed in this study. The technique is known to be effective for high-frequency (>0.1 Hz) ground-motions required for structural engineering purposes. The approach has been widely and successfully used in different parts of the globe. This approach is based on introducing dynamic corner frequencies. This method requires a detailed knowledge of the path and site effects; Input parameters are based on the characteristics of both the source and the path (seismic velocities and attenuation in the crust). The path attenuation is quantified by the quality factor, Q-value, and geometric spreading function. In this study, the quality factor evaluated in this region by Shanaki et al. (2011) [21] was used. The modelling considers Shear-wave velocity, crustal density, rupture propagation speed, fault-rupture dimensions, focal mechanism, seismic moment or magnitude, stress drop, slip distribution, hypocentral distance (or epicentral distance), focal depth, and fault pulsing percentage. The stress drop controls the amplitudes of high frequency radiation while the fault pulsing percentage influences the relative amount of low frequency radiation (Motazedian and Atkinson 2005) [22]. At high frequencies, the acceleration spectral amplitude decreases rapidly; this has been modelled with the spectral decay factor κ. Its site component, $\kappa 0$, is used here as input parameter. In this paper, the simulation program EXSIM, which is suggested by Motazedian and Atkinson (2005) [23] was used. The essential input parameters given to the simulation program are shown in table 3.

Table 3. Input parameters used in simulation of Sefid Sang earthquake.

Parameter	Value
Shear-wave velocity (v_s)	*3.2 Km/s*
Crustal Density (ρ)	*2.8 gr/cm^3*
Quality factor Q	$Q = 91f^{0.88}$
κ_0	*0.005 S*
Rupture propagation speed ($0:8v_s$)	*2.56 Km/s*
Stress parameter	*8 bars*
Fault length and width	*L= 10Km; W=8Km*
Type of sub fault	*Static (constant corner frequency for all sub faults)*

After simulating the earthquake by applying EGF and SFF methods; the observed records and the simulated graphs by these two techniques, were compared. The comparison of the observed and synthetic diagrams of acceleration is demonstrated in Figure 5. There is a good agreement between the main characteristics of the observed and simulated ground motions. However, the simulated ground motions can mostly explain major characteristics of the observed records.

We present the results of the simulations and their comparisons with the observed Fourier and Response spectra of the earthquake in Figure 6. In general, the synthetics are in good agreement

with observations in almost all cases, considering inherent limitations of the methods and their simplicity. Also, the peak values of the observed and simulated records of the main event are shown in table 4.
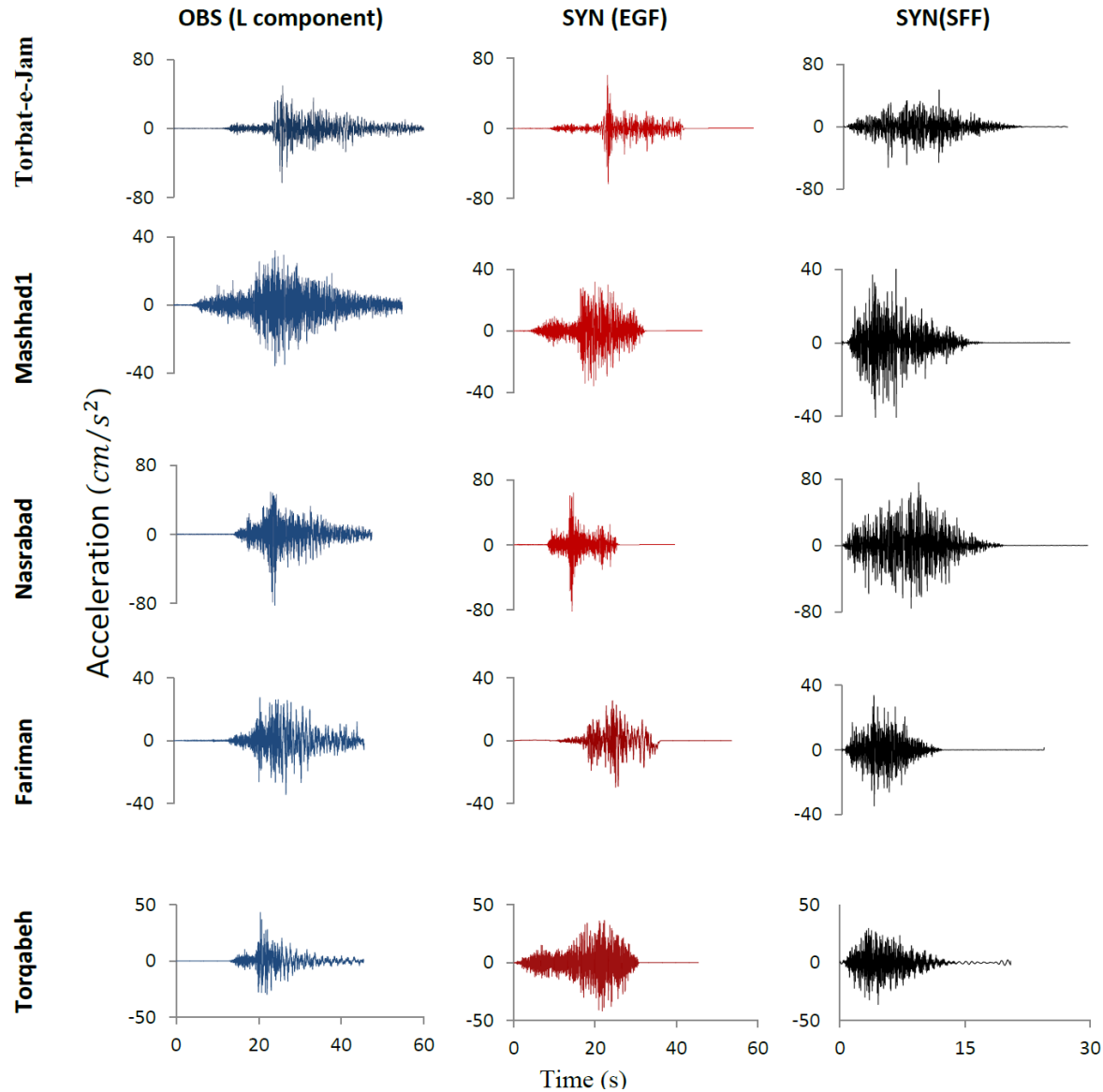

Figure 5. Observed (obs) and synthetic (syn) acceleration diagrams of the main event in Longitudinal (L) component of the near field stations.
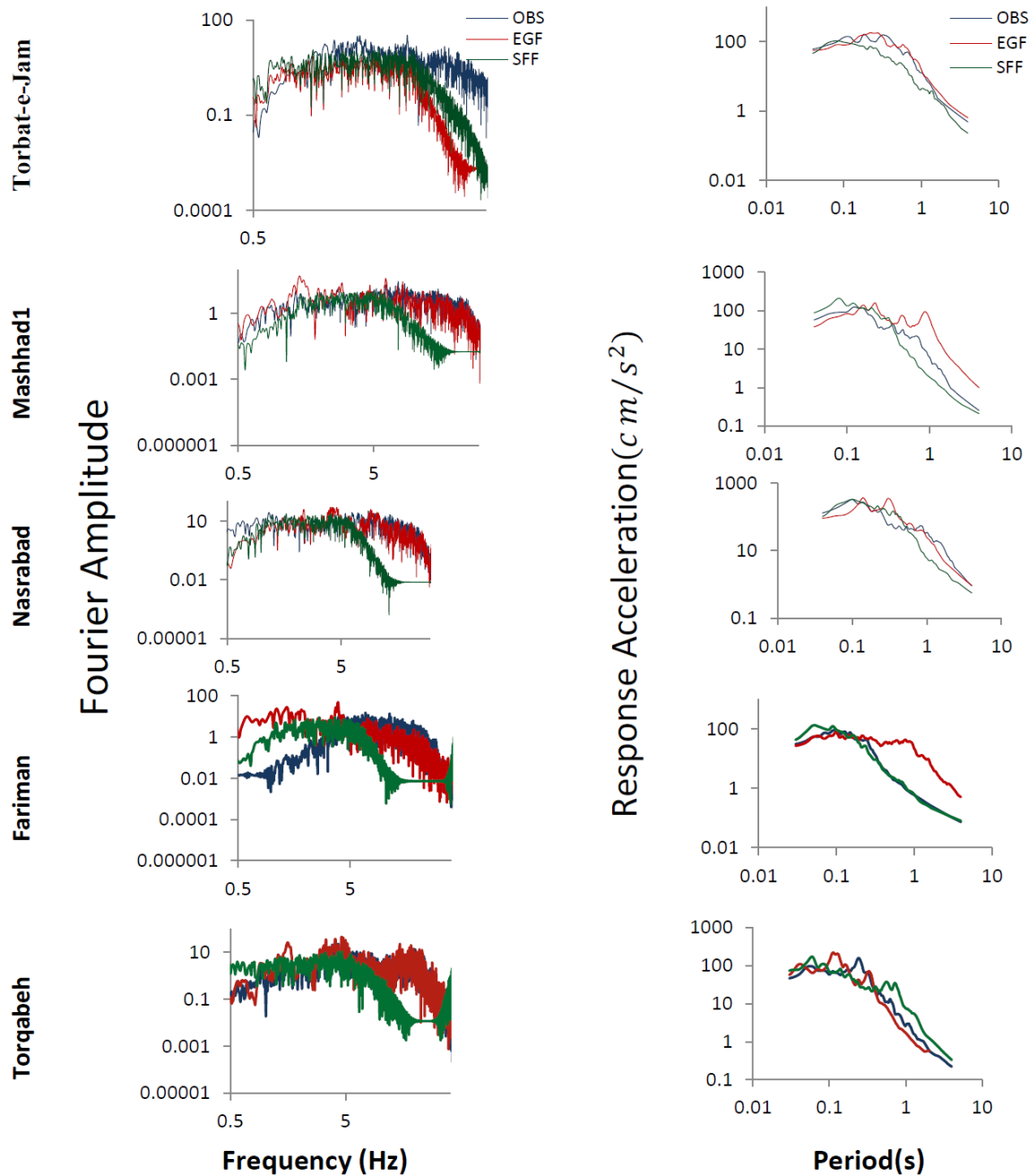
Figure 6. Observed and synthetic Fourier and acceleration response spectra of the main event in L component of the stations.

Table 4. The peak values of the observed and simulated diagrams of the earthquake in three components

station	parameter	Observed			Synthetic(SFF)	Synthetic(EGF)		
		L	T	V		L	T	V
Torbat-e-Jam	PGA(cm/s²)	63.02	55.16	32.15	52.14	63.16	55.36	29.12
	PGV(cm/s²)	3.20	2.17	1.24	0.92	3.59	3.06	1.15
	PGD(cm/s²)	0.19	0.14	0.07	0.04	0.20	0.17	0.08
	Duration(S)	16	17	24	9	13	14	21
Mashhad 1	PGA(cm/s²)	37.70	35.80	21.15	45.07	37.65	35.73	21.54
	PGV(cm/s²)	1.16	1.00	0.59	0.62	2.43	1.45	0.88
	PGD(cm/s²)	0.06	0.08	0.04	0.01	0.31	1.09	0.09
	Duration(S)	19	20	24	7	14	14	16
Nasrabad	PGA(cm/s²)	87.41	112.04	45.36	90.92	87.32	112.27	45.21
	PGV(cm/s²)	2.04	2.90	1.32	1.58	3.61	4.74	1.86
	PGD(cm/s²)	0.28	0.11	0.08	0.04	0.27	0.36	0.09
	Duration(S)	16	14	24	9	16	19	22
Fariman	PGA(cm/s²)	34.30	30.20	23.80	34.80	30.60	28.70	21.30
	PGV(cm/s²)	3.21	2.91	1.83	0.48	5.62	3.5	2.79
	PGD(cm/s²)	0.45	0.36	0.12	0.01	0.57	0.50	0.24
	Duration(S)	22	23	25	6	14	13	18
Torqabeh	PGA(cm/s²)	43.20	37.40	17.80	36.05	41.70	33.70	17.00
	PGV(cm/s²)	1.11	0.81	0.41	1.20	2.15	2.32	0.56
	PGD(cm/s²)	3.20	1.12	0.18	0.12	3.71	1.19	0.46
	Duration(S)	15	26	29	8	20	20	20

5. Conclusions

In this study, the empirical Green function method was successfully applied in simulating strong ground motion. According to the above results, the EGF provides a good alternate for the ground motion simulation in Khorasan-e-Razavi region. On one hand, EGF method compared with other deterministic techniques has the advantage of not requiring to compute numerically the propagation and local site effects (Kamae et al. 1998; Kamae and Irikura 1998) [24-25]; on the other hand, its main limitation is that it can be applied only in cases where appropriate records of small events in the source area, which are considered as Green functions, are available. Unfortunately, it is rare to have good records of such small events, especially in the source area of a future large earthquake; also in some of the applications of the empirical Green function method, a detailed description of the source rupture process is required while some of these parameters are poorly constrained. Therefore, for practical simulation purposes, a more appealing approach is one in which a detailed description of the source process of a future earthquake is not required (Ordaz et al. 1995) [27]. As an alternative way to avoid this limitation, we propose the use of the stochastic finite-fault modeling. The stochastic finite-fault method requires a detailed knowledge of the path and site effects but less information about the source process.

The stochastic simulation method is effective at predicting ground motions from a large earthquake, especially for regions where the absence of small magnitude event records precludes the application of the EGF method. We tested the technique by comparing the synthetic and the recorded motion from the Sefid Sang earthquake (Mw=6.1). The comparison suggests that this method is effective at simulating near source ground motions in a broad-frequency range of engineering interest. However, the results achieved from applying EGF method have better agreement with the observed ones; since, records of small earthquakes used as empirical Green functions inherently include propagation and site effects, so that uncertainties associated with the crustal structure and local geology are eliminated (Hartzell 1978, 1992) [8-28]. In addition, incorporation of site amplification effects on stochastic method is usually one of the most troublesome tasks, because site-specific geotechnical information is usually limited or nonexistent. The simulated strong ground motions in comparison with the observed ones show a good agreement although some waveforms are underestimated or overestimated. This results show that the strong ground motions can be explained by the average fault rupture model.

The estimated fault plane solution shows reverse mechanism with strike-slip component for this event, the fault caused this earthquake is determined as a reverse oblique fault (mostly compressional with a small strike slip component with North West-South East fault trend). Strike, dip and rake of causative fault of the earthquake were determined as 311, 55 and 117 degrees, respectively.

Considering the fault plane and distribution of aftershocks, the rupture initiated from the element (1, 2) on the fault surface at the depth of 11 km and propagated from hypocenter from North West to South East direction. The duration of the rupture in this event was more than 18 seconds.

April 5, 2017 earthquake was one of the several events with magnitude greater than 6 that have occurred in this region; such seismic events at a distance close to major cities such as Mashhad would cause massive destruction and loss of lives. Therefore, the ground motion characteristics during the main shocks should be considered for the high safety design of the damaged area.

6. References

[1]- Berberian, M, 1983,**Continental deformation of Iran plateau**, Geological survey of Iran 52: 19-68.

[2]- Berberian, M., Jackson, J. A., Qorashi, M., Talebian, M., Khatib, M. and Preistley, K., 2000, **The 1994 Sefidabeh earthquakes in eastern Iran: blind thrusting and bedding – plane slip on a growing anticline, and active tectonics of the Sistan suture zone**, Geophysical Journal International, 142: 283-299.

[3]- Arjmand, M. R., Kangi, A., Hafezi Moghadas, N., 2019, **The effect of Tous fault on groundwater resources in northern parts of Mashhad plain**, Iranian Journal of Earth Sciences, 11: 205-214.

[4]- Miyake, H., Iwata, T., and Irikura, K., 2000, **Source characterization of Inland crustal earthquakes for near- source ground motions**, Proceedings of the 6th international conference on seismic zonation.

[5]- Zafarani, H., 2012, **A Hybrid Empirical-Stochastic Method for Ground Motion Simulation; A Sample Study: The 22 February 2005 (MW 6.4) Zarand (Central Iran) Earthquake**, 15 WCEEAt, Lisbon, Portugal.

[6]- Rahimi Bahoosh, H., and Hamzehloo, H., 2011, **Simulation of strong ground motion for the 2004 Firozabad   Kojoor earthquake in northern Iran**, Iranian Journal of Geophysics, 5: 1-13.

[7]- Kanth, S., R., 2008, M**odeling and synthesis of strong ground motion**, Journal of earth system science, 117: 683-705.

[8]- Hartzell, S. H., 1978, **Earthquake aftershocks as Green functions**, Geophysical Research Letters, 5: 1-4.

[9]- Mueller, C., 1985, **Source pulse enhancement by Deconvolution of an empirical Green function**, Geophysical Research Letters, 12: 33-36.

[10]- Hutchings, L., and Viegas, G., 2012, **Application of Empirical Green Functions in earthquake source, wave propagation and strong ground motion studies**, Lawrence Berkeley National Laboratory, USA 3: 80-130.

[11]- Cheng, F., and Huang, H., 2011, **Strong ground motion simulation of the October 22, 1999 Chiay earthquake using hybrid Green function method**, 4th IASPEI international symposium, Santa Barbara, USA.

[12]- Courboulex, F., Virieux, J., Deschamps, A., Gilbert, D., and Zoll, A., 1996, **source investigation of a small event using empirical Green functions and simulated annealing**, Geophysical Journal International, 125: 768-780.

[13]- Irikura, K., 1991, **The physical basis of the empirical Green function method and the prediction of strong ground motion for large earthquake**, International workshop of seismology and Earthquake Engineering.

[14]-Wells, D., and Coppersmith, K., 1994, **New empirical relationships among magnitude. rupture length, rupture width, rupture area and surface displacement**, Bulletin of the Seismological Society of America, 8: 974-1002.

[15]- Irikura, K., 1983, **Semi-empirical estimation of strong ground motions during large earthquakes**, Bulletin of the Disaster Prevention Research Institute, 33: 63-104.

[16]- Irikura, K., 1986, **Prediction of strong acceleration motions using empirical Green function**, 7th Japan Earthquake Engineering Symposium 151-156.

[17]- Boore, D., M., 1983, **Stochastic simulation of high-frequency ground motions based on seismological models of the radiated spectra**, Bulletin of the Seismological Society of America, 79: 1865–1894.

[18]- Boore, D., M., 2003, **Prediction of ground motion using the stochastic method**, Pure and Applied Geophysics, 160: 635–676.

[19]- Sengupta, P., 2012, **Stochastic finite-fault modeling of strong earthquakes in Narmada South Fault, Indian shield**, Journal of Earth System Science, 121: 837–846.

[20]- Motazedian, D., and Atkinson G., M., 2005a, **Stochastic finite-fault modeling based on a dynamic corner frequency**, Bulletin of the Seismological Society of America, 95: 995–1010.

[21]- Shanaki, S., Gheitanchi, M., R., Abrehdari, H., and Miraj, k., 2011, **Evaluation of Quality factor beneath local seismic network in NE Iran**, Journal of The Earth, 21: 51-60.

[22]- Motazedian, D., and Atkinson, G. M., 2005b, **Earthquake magnitude measurements for Puerto Rico**, Bulletin of the Seismological Society of America, 95: 725– 730.

[23]- Motazedian D., and Atkinson, G. M., 2005c, **Ground-motion relations for Puerto Rico**, Geological Society of America, 385: 61–80.

[24]-Kamae, K., Bard, P., Y., and Irikura, K., 1998, **Prediction of strong ground motion in a EURO-SEISTEST using the empirical Green's function method**, Journal of Seismology, 2:193-207.

[25]- Kamae, K., and Irikura, K., 1998, **Source model of the 1995 Hyogo-ken Nanbu earthquake and simulation of near-source ground motion**, Bulletin of the Seismological Society of America, 887: 400-412.

[26]- Atkinson, G., M., and Boore, D. M., 2006, **Earthquake ground-motion prediction equations for eastern North America**, Bulletin of the Seismological Society of America, 96: 2181–2205.

[27]- Ordaz, M., Arboleda, J., and Singh, S. K., 1995, **A scheme of random summation of an empirical Green's function to estimate ground motions from future large earthquakes**, Bulletin of the Seismological Society of America, 85: 1635 –1647.

[28]- Hartzell, S. H., 1992, **Estimation of near-source ground motions from a teleseismically derived rupture model of the 1989 Loma Prieta, California, earthquake**, Bulletin of the Seismological Society of America, 82: 1991– 2013.